JOURNAL OF MATERIALS SCIENCE 32 (1997) 301–308

Diffusion of water within an amorphous carbohydrate

B. J. ALDOUS*, F. FRANKS
Pafra Ltd (Biopreservation Division), 150 Science Park, Milton Road, Cambridge, CB4 4GG, UK

A. L. GREER
University of Cambridge, Department of Materials Science & Metallurgy, Pembroke Street, Cambridge, CB2 3QZ, UK

The evaporative drying of solid amorphous Ficoll–water mixtures is studied by thermogravimetric analysis. Differential scanning calorimetry is used to determine the physical state (glass or visco-elastic rubber) from which drying is performed. Drying is observed to continue at temperatures far below the glass-transition temperature (T_g), showing that water is mobile within amorphous carbohydrate matrices. Two models for drying kinetics are tested, and it is found that the rate of water removal is limited by diffusion through the amorphous matrix and not by desorption from the surface of the material. Although the viscosity of carbohydrate–water glasses has previously been found to obey Williams–Landel–Ferry kinetics, the drying process was found to follow Arrhenius kinetics both above and below T_g. In the glass-transition region the water diffusivity is not strongly dependent on the water content, and Fickian kinetics are observed.

1. Introduction

Drying has long been used as a method for the preservation of foodstuffs and pharmaceuticals [1]. For the maximum preservative action it is essential that the solid material formed on drying is amorphous rather than crystalline. The natural degradation processes of proteins in food or pharmaceuticals are greatly retarded, even stifled, when the proteins are trapped in a rigid amorphous matrix, most commonly based on a carbohydrate–water mixture. On the other hand, if crystallization occurs during drying, there is harmful partitioning of salts between the crystalline and liquid/rubbery phases, and water rejected from the crystals can increase mobility in the remaining untransformed matrix, accelerating the crystallization. Such processes are frequently seen in freeze-drying of products containing low molecular weight sugars such as mannitol, and in some foods with intermediate water content, an example being the staling process for starches in bread.

In recent years, there has been particular interest in evaporative drying of carbohydrate–water mixtures to stabilize labile pharmaceuticals [1]. The prospects for application are good, as the amorphous solids so formed are very stable and offer substantially improved shelf lives for the embedded agents. The carbohydrates chosen must be compatible with the embedded proteins and must be resistant to crystallization. An example is the sucrose-based polymer, Ficoll [2], which is used in the present work; Ficoll is cross-linked and unable to crystallize. In applying such materials, the processes of drying (to preserve) and rehydration (to re-activate) are central. Also, there is residual water in the amorphous solids and it acts to increase molecular mobility, and permit some reactions. For these reasons it is crucial to characterize the diffusion of water in such carbohydrate–water amorphous solids. There have been several studies, based on nuclear magnetic resonance spectroscopy (NMR), of the rotational mobility of water in carbohydrate matrices (e.g. [3, 4]), but only a few studies (e.g. [5]) of long-range diffusion and drying. These are the focus of the present work.

2. Molecular mobility in carbohydrate–water glass-forming systems

Concentrated aqueous solutions of carbohydrates can, on dehydration or cooling, form amorphous solids (glasses). On heating such systems a classical glass transition is observed, for example a temperature-dependent viscosity of the kind illustrated schematically in Fig. 1, and changes in specific heat (Fig. 2). The residual water in the glass acts in the same manner as a plasticizer in a glassy polymer [4], increased water content lowering the glass-transition temperature T_g. In reviewing the literature relevant for the present work it is useful to include some studies on

* To whom correspondence should be addressed.

0022–2461

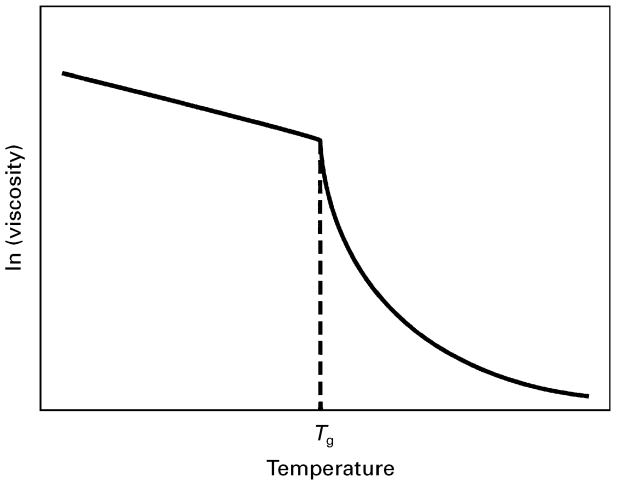

Figure 1 A schematic diagram of the temperature dependence of viscosity in a "fragile" glass-forming system, such as carbohydrate–water. There is a clear break in behaviour at the glass transition temperature T_g. At temperatures just above T_g the temperature dependence of viscosity is very strong and not Arrhenian.

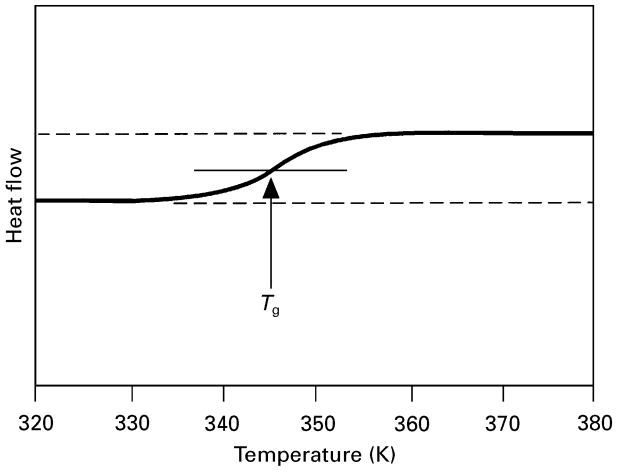

Figure 2 Differential scanning calorimetry trace (heating rate $10^\circ\,min^{-1}$) of a Ficoll–water glass of water content 4.7 wt %. The heat flow is proportional to the specific heat and the mass of the sample. The sample has been given a standard pre-treatment of cooling to $-23\,^\circ C$, heating to $127\,^\circ C$ and cooling to $-23\,^\circ C$ (all at $10^\circ\,min^{-1}$). The dashed lines show the construction used to define the glass-transition temperature.

polymers; these are particularly helpful in pointing out how diffusion behaviour can vary with the molecular size of the diffusing species.

It is characteristic of "fragile" [6] glass-forming systems that on cooling, the viscosity rises markedly as T_g is approached. The temperature dependence of the viscosity, η, is not Arrhenian, and is often described by Vogel–Tammann–Fulcher (VTF) kinetics

$$\eta = \eta_0 \exp\left(\frac{C}{T - T_0}\right) \qquad (1)$$

where η_0 and C are constants, and T_0 is the ideal glass-transition temperature, somewhat lower than the measured temperature T_g. For polymers, the viscosity is most commonly described by Williams–Landel–Ferry (WLF) kinetics

$$\eta = \eta_g \exp\left[\frac{-C_1\ (T - T_g)}{C_2 + (T - T_g)}\right] \qquad (2)$$

where C_1 and C_2 are constants, and η_g is the viscosity at T_g. These two descriptions are very closely related [7–9]. In carbohydrate–water systems, in the rubbery state above T_g, VTF or WLF kinetics have been found for viscosity [9], ^{13}C NMR relaxation times [10], and devitrification rates [11]. In each case, the mobility sampled is that of the carbohydrate molecules. In the present work, however, it is the mobility of the water which is of concern.

Ehlich and Sillescu [8] showed that for large dye molecules (molecular weight $\approx$250) in polymers, the diffusivity above T_g showed WLF kinetics, as for viscosity. For smaller molecules, on the other hand, the kinetics were Arrhenian. In the latter case the Arrhenian behaviour continued through T_g, with some increase in activation energy above T_g being found only for relatively slow diffusants. It appears that for large molecules the diffusivity and viscosity are linked by the Stokes–Einstein relation. For small molecules in large molecule-based glasses, however, they become decoupled, with the diffusivity at low temperature being much greater than would be expected from the viscosity of the glass.

Water in carbohydrate–water glasses behaves, as would be expected, as a small molecule. NMR studies by Girlich [3] on sucrose–water mixtures showed that the temperature dependence of the rotational mobility of water is clearly different from that of sucrose. At the glass-transition temperature Girlich observed that both the rotational and translational diffusion of sucrose ceased but the rotational diffusion of water continued at temperatures far below T_g. Parker and Ring [5] have shown that for maltose–water close to T_g, the diffusion of water has Arrhenian kinetics. Oksanen and Zografi [4] performed both diffusion and proton-NMR relaxation measurements for water in poly(vinylpyrrolidone). They found that the translational diffusivity of water was still high ($\sim 10^{-12}\,m^2\,s^{-1}$) at room temperature, though not as high as in pure water. In these studies the diffusivity of water was higher in glasses with higher water content, but the dependence was weak, especially in very dry samples. Noel and co-workers [12] have explored the consequences of this characteristic behaviour of water on reaction kinetics in carbohydrate–water systems.

The present work focuses on drying kinetics. There has been much work on whether the rate of loss of a small molecule is controlled by its diffusivity. In some starches, porosity develops on drying, and analysis of the effective diffusivity is complex, as vapour-phase diffusion in the voids plays a significant rôle [13]. Even when such effects do not arise, drying kinetics can be complex. For example Pikal *et al.* [14] found that a plateau level of water was reached; they concluded that for the amorphous materials in their study, the rate-limiting process in drying was probably evaporation at the sample surface. As pointed out in [14], a "plateau" effect could also arise when the

diffusivity is very dependent on water content; in that case a hard surface layer would form, diffusion through which would be rate-controlling. Consequences are non-Fickian diffusion profiles and time-dependent effects. Such behaviour has been studied in polymeric systems, for example for the diffusion of methanol in poly(methylmethacrylate) [15]. However, there are examples in which simple Fickian behaviour is found. An example particularly relevant for the present work is in the drying of maltose–water [5].

3. Materials and methods

3.1. Preparation of Ficoll–water glasses

Ficoll [2], a cross-linked sucrose co-polymerisate, was selected as a model material for study as it is water-soluble, and able to vitrify at temperatures well above room temperature. Furthermore, it is unable to crystallize, as the sucrose chains are cross-linked, leading to a very stable glassy matrix. The Ficoll–water glasses were produced from aqueous solutions by evaporative drying in a vacuum oven. Ficoll 400, of average molecular weight 400 000 was made into $\sim$30 wt % solutions which were poured into trays of aluminium foil, giving a solution depth of 5 to 8 mm. After allowing any air bubbles to be removed, the trays were loaded into a vacuum oven (volume 3×10^{-4} m^3, with a Heto CT-60 cold trap of 1 l capacity, and a Javac DD-75 double-stage vacuum pump of displacement 4.5 m^3 h^{-1}). The pressure inside the oven was held at 2 kPa using a needle-valve controlled air bleed. This pressure was selected to prevent bubbling of the carbohydrate solution. The temperature of the oven was maintained at 30 to 40 °C until the Ficoll–water mixture formed a glass, i.e. until the glass transition temperature of the mixture exceeded 40 °C. To increase the rate of drying, the temperature of the oven was then ramped slowly up to 90 °C. No browning of the glass was observed. In the dried form the thickness of the glass had reduced to 0.5 to 1 mm. As expected, examination by optical microscope showed no crystallization. There was no evidence for cracking or for the development of porosity in the dried samples; thus diffusion of water should be through the glassy matrix without interference from defects, for example of the kind discussed in [13].

Samples were cut from the aluminium trays with a scalpel and their thickness measured with a micrometer. The samples were then divided into two pieces (for analysis, one by thermogravimetric analysis (TGA), the other by differential scanning calorimetry (DSC)) and stored separately in stoppered glass vials.

3.2. Thermogravimetric analysis

TGA was performed with a Perkin-Elmer TGA 7 analyser. The TGA 7 furnace was calibrated for temperature using alumel and nickel standards (Curie points 163 °C and 354 °C, respectively). The balance was then calibrated for weight with a 100 mg standard. All analyses were performed under a constant flow of dry, oxygen-free nitrogen. The Ficoll–water glass sample was cut to the shape of the platinum sample pan and weighed in the analyser. Typically samples have weight 15 to 30 mg, area 0.25 cm^2 and thickness 0.5 to 1 mm. The weight of the sample was then recorded while it was subjected to a heating programme. After analysis the sample was quickly removed from the analyser and sealed in a stoppered glass vial.

3.3. Determination of water content

Water contents were determined only after TGA. Karl Fischer coulometric titration was performed using a Mitsubishi CA-05 moisture meter equipped with Hydranal A and C reagents (Riedel de Haën). About 30 ml formamide was poured into a glass vial which was then sealed with a rubber stopper. Portions (0.5 ml) of this were then transferred to the moisture meter using a Hamilton gas-tight syringe, and the water content was determined. A syringe was then used to add 1 ml of this formamide of known water content to the glass samples after TGA. The vials were warmed to 85 °C on a Techne DB-2A Dri-block heater until all the carbohydrate glass had dissolved. The water content was determined using 0.25 ml portions of the resulting solution analysed in the moisture meter. The water content of the glass was obtained by subtracting the water content of the formamide. From the weight loss during TGA, the final weight of the sample, and the water content determined by the Karl Fischer analysis, the original water content of the glass before TGA was calculated. The error in the water content determination is estimated to be $\pm$0.1 wt %.

3.4. Differential scanning calorimetry

For each sample analysed by TGA, its companion was analysed by DSC to determine its glass transition temperature (T_g) and thereby infer its initial state (glass or visco-elastic rubber). The calorimetry used a DSC-2 instrument (Perkin-Elmer) with a DARES-DSC [16] data capture system. To prevent any water loss, the sample was loaded into a pre-weighed, large capacity stainless steel pan and hermetically sealed with a lid and "O" ring. After weighing, the filled sample pan was loaded into the calorimeter and equilibrated at 27 °C.

The glass transition temperature, as measured by DSC, is affected by the thermal history of the sample (e.g. rate of cooling from the melt and subsequent ageing processes) and by the heating rate on analysis. These phenomena are well known [e.g. 17]. To eliminate such effects and relate T_g only to sample composition, it is necessary to standardize the thermal history of the samples. To do this, the samples were loaded into the calorimeter at 27 °C, cooled at 10° min^{-1} to $-$23 °C (a temperature certainly below T_g), and then warmed at 10 ° min^{-1} to 127 °C (a temperature above T_g). On subsequent re-cooling to $-$23 °C at 10° min^{-1}, the glass is formed in a controlled and reproducible manner. Immediately after the cooling run had stopped, the sample was re-heated at a standard rate of 10° min^{-1} and the power–time curve recorded; an example is shown in Fig. 2. As there was no significant interval between cooling and re-heating,

there was no time for ageing processes to occur that might affect the determination of T_g. All samples were analysed by this method, permitting direct comparison of the thermal analysis data for all samples.

4. Results and discussion

4.1. Isothermal drying of Ficoll–water glass below T_g

The kinetics of isothermal drying were measured for several samples. The dependences of the kinetics on water content and on drying temperature are considered in later sections. Here the data for one case are considered as an example: a sample of Ficoll–water glass ($T_g = 89\,^{\circ}C$) held at $30\,^{\circ}C$ in the TGA under flowing nitrogen for 17 h. The resulting weight–time profile (Fig. 3) shows a weight loss from 7.994 mg to 7.898 mg, representing a fall in water content from 4.3 wt % to 3.1 wt %. This loss is assumed to be totally due to the loss of water from the glassy matrix. The 25% reduction cannot be accounted for by the loss only of water adsorbed on the surface of the sample. The glass did not discolour (brown) during the further drying in the TGA and it is therefore assumed not to have decomposed. The monotonic weight loss over the long drying period suggests that water continually diffuses to the surface of the glass before being removed by the dry nitrogen stream. Although the rate of water loss is very low, it is clear that water is able to diffuse through the glassy matrix at measurable rates at temperatures more than 50° below the glass transition temperature. Fig. 3 shows that the rate of water loss slows during the experiment. This could have several causes:

(i) a reduction on diffusion coefficient (related to water content and T_g);

(ii) a reduction of water concentration gradients in the sample; or

(iii) a reduction in the desorption rate as the water content of the sample surface drops.

In the following section a kinetic analysis is undertaken to distinguish between these possibilities.

4.2. Models for the rate of water loss

To analyse the kinetics of water removal from a Ficoll–water glass, two models were tested to determine whether the rate of water loss is limited by desorption from the surface of the glass or by diffusion through the glass matrix.

In the first model it is assumed that the rate of water loss is controlled by the rate of desorption or evaporation from the surface. Since diffusion inside the glass is not rate-limiting, the concentration gradients would be small. In the ideal case, illustrated in Fig. 4, it is assumed that the water content in the glass always remains uniform. Water is lost from the glass through its top and bottom surfaces. The rate of water removal is taken to be proportional to the difference in water concentration across the surface. Taking the water content of the dry nitrogen gas to be zero, the rate of removal is simply proportional to the water content x (wt %) of the glass

$$\frac{dx}{dt} = -kx(t) \qquad (3)$$

where t is time and k is a constant. This exponential decay in water content would give linear plots of $\ln(x/x_0)$ versus t.

In the second model, it is assumed that the rate-limiting process is the diffusion of water through the glass matrix to the surface. Ideally, the water content in the glass at the surface would be zero and diffusional concentration profiles would be set up within the glass, as illustrated schematically in Fig. 5. Again,

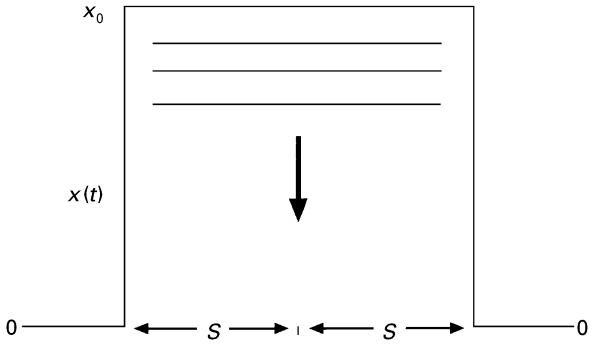

Figure 4 Drying of a plate of carbohydrate–water glass when desorption of water from the plate surfaces is rate-limiting. Schematic profiles are shown for the water content through the thickness of the plate; water is removed through the surfaces of the plate (at left and right).

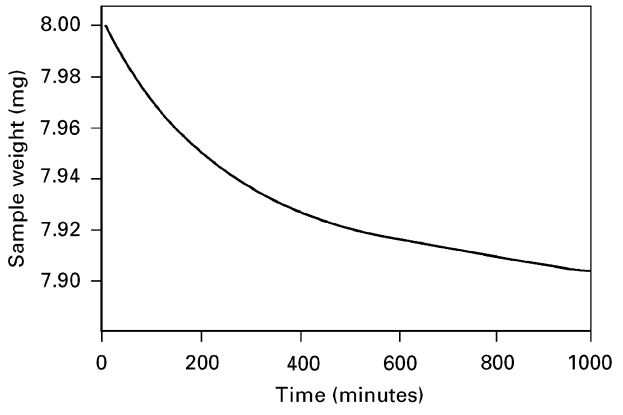

Figure 3 Thermogravimetric analysis trace for a Ficoll–water glass held at $30\,^{\circ}C$ for 17 h. The weight loss corresponds to drying from an initial water content of 4.3 wt % to 3.1 wt %.

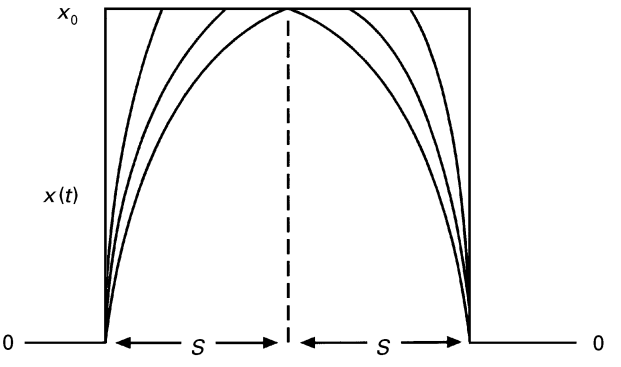

Figure 5 Drying of a plate of carbohydrate–water glass when diffusion of water through the plate is rate-limiting. Schematic profiles are shown for the water content through the thickness of the plate; water is removed through the surfaces of the plate (at left and right).

water is lost through the top and bottom surfaces of the sample. In the early stages of drying, before the diffusional profiles from the opposite surfaces meet in the middle, a simple solution of the diffusion equation can be applied [18] when the water diffusion coefficient D is assumed constant. The total water loss $(x_0 - x)$ is given by

$$\left[\frac{(x_0 - x)}{x_0}\right]^2 = \frac{4}{\pi S^2} D\,t \qquad (4)$$

where x_0 is the original water content (wt %) of the sample and S is the half-thickness of the sample. Equation 4 has a quite different form from Equation 3, permitting the two models to be readily distinguished from measurements of the rate of water loss.

Seven pieces of Ficoll–water glass were cut from a single sample of initial water content 4.8 $\pm$ 0.6 wt %. The water loss was then monitored by isothermal TGA at 30, 40, 50, 60, 70, 80 and 90 °C. Fig. 6 shows plots of $\ln(x/x_0)$ versus t, which should be linear if the first model is obeyed. Fig. 7 shows plots of $[(x_0 - x)/x_0]^2$ versus t, which should be linear if the second model is obeyed. Clearly the second model fits the data much better, i.e., the rate of water loss from the samples appears to be limited by the diffusion of water through the samples. The gradients of the plots in Fig. 7 are proportional to the diffusion coefficient (gradient $= (4/\pi S^2)D$). It can be seen that the diffusion coefficient is constant, to a good approximation. It does, however, tend to decrease as the water loss continues. In the early stages of drying there could be transient effects associated with non-uniform water content in the samples. At longer drying times a potential explanation for the non-linearity in the plots would be that the diffusion profiles from each surface would meet and the simple kinetics of Equation 4 would no longer be obeyed. As discussed for example in [19], the deviation occurs when $2S \approx 3(Dt)^{1/2}$, corresponding to the loss of ~75% of the original water content of the sample. For the data in Fig. 7, even for the longest drying time at the highest temperature, only ~50% of the original water is lost; therefore, if the diffusivity is constant, Equation 4 should remain a good approximation. A further reason for non-linearity in the plots in Fig. 7 is the finite area of the sample plates. The resulting edge effects are, however, expected to be negligible as the lateral dimension of the plates is one order of magnitude greater than their thickness. Thus the observed decreases in diffusivity are likely to be real, and they are analysed in section 4.5.

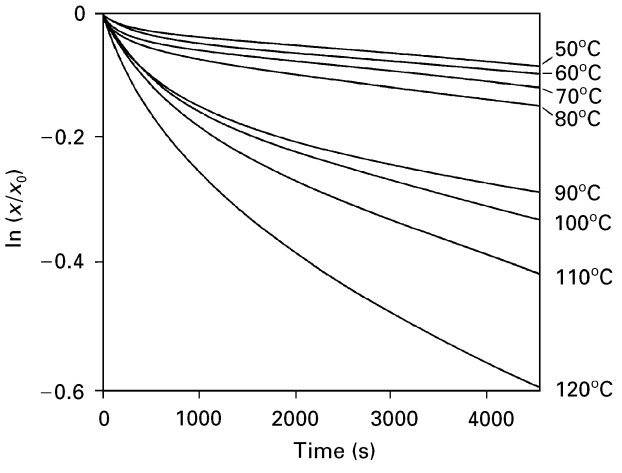

Figure 6 Drying profiles (from isothermal TGA data as in Fig. 3) plotted as $\ln(x/x_0)$ versus t for a series of samples cut from Ficoll–water glass of initial water content 4.8 $\pm$ 0.6 wt % (x is the water content in wt %, x_0 the initial water content, and t time). For each sample the corresponding drying temperature is shown on the profile. These plots should be linear if the rate of drying of the glass is limited by the desorption of water from its surfaces.

4.3. Temperature dependence of the diffusion coefficient

Having established in section 4.2 that the rate of water loss is diffusion-controlled, the diffusivity of the water can be studied. Fig. 7 shows that the diffusivity D is approximately constant as a given sample dries. Average values of D for each drying temperature are obtained by fitting straight lines to the data in Fig. 7. The temperature dependence of these values is displayed in Fig. 8. This shows Arrhenius behaviour, with an

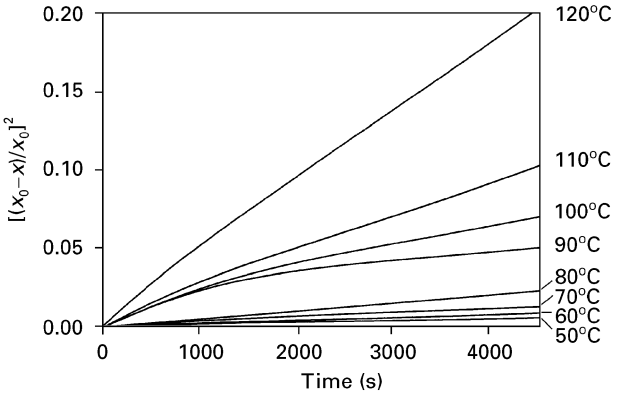

Figure 7 Drying profiles (from the same isothermal TGA data as Fig. 6) plotted as $[(x_0 - x)/x_0]^2$ versus t. These plots should be linear if the rate of drying of the glass is limited by the diffusion of water through the glass. The gradient of these lines is $(4/\pi S^2)D$, where S is the half-thickness of the plate of Ficoll–water glass and D is the water diffusivity. The samples at 50, 60 and 70 °C are in the glassy state, the others in the rubbery state.

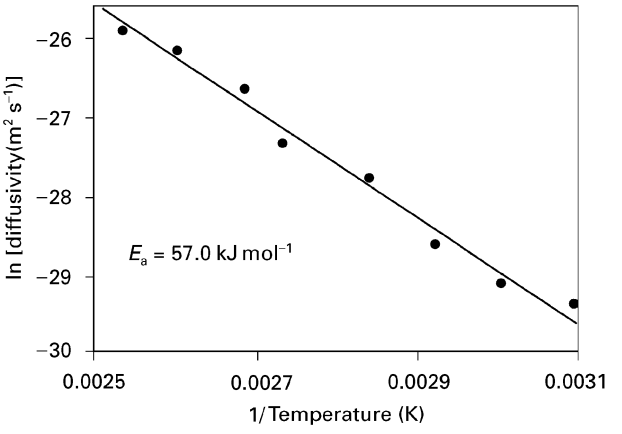

Figure 8 Arrhenius plot of the water diffusivity D as a function of temperature. The D values are obtained from the slopes of straight lines fitted to the curves in Fig. 7.

activation energy of $57 \pm 5\ \mathrm{kJ\,mol^{-1}}$. The error in the D measurements ($\pm 10\%$) comes mainly from the non-uniformity of sample thickness and the uncertainties in its measurement.

It is of interest to compare the apparent activation energies for water diffusion at different stages of drying. This can be done by determining the times for loss of a given fraction of the original water content. Except at the start, the activation energy is found, within experimental error, to be constant throughout drying, the value matching that determined above. In the early stages of drying, the apparent activation energy is slightly less, being $48 \pm 5\ \mathrm{kJ\,mol^{-1}}$ for 5% water loss.

4.4. Relationship between T_g and water content

Differential scanning calorimetry (Fig. 2) is used to determine the glass-transition temperature T_g, and the correlation of T_g with water content is shown in Fig. 9. For each water content there is a significant spread in T_g values; none the less a clear glass-transition region can be identified. Having identified this region, it is possible to see whether the diffusion data correspond to samples in the rubbery or glassy states. In Fig. 7, for example, the samples drying at $\leqslant 60\,^{\circ}\mathrm{C}$ are in the glassy state, those at $\geqslant 80\,^{\circ}\mathrm{C}$ in the rubbery state. At $70\,^{\circ}\mathrm{C}$ the initial state is rubbery, but as drying proceeds the glassy state is very soon entered. There is no evident change in behaviour in the glass-transition region. Any change, however, might be somewhat blurred by the non-uniform water contents of the drying samples.

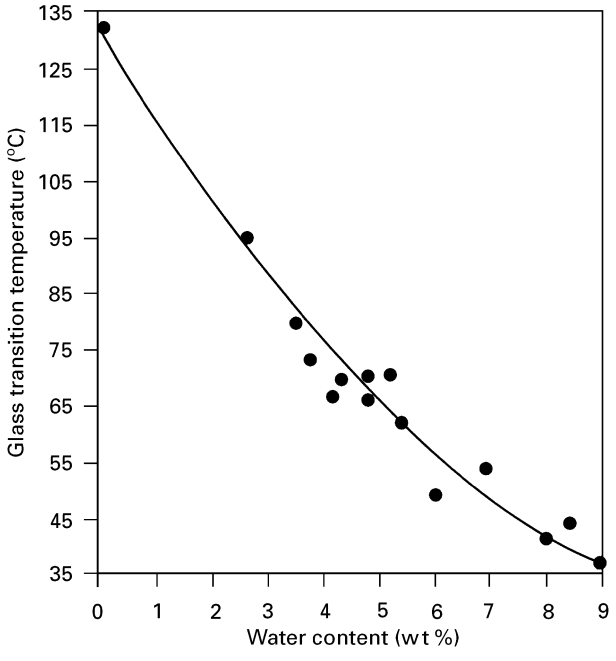

Figure 9 The glass-transition temperature T_g of Ficoll–water samples (determined using DSC, as shown in Fig. 2) as a function of water content (determined by Karl Fischer analysis). The line is a guide for the eye.

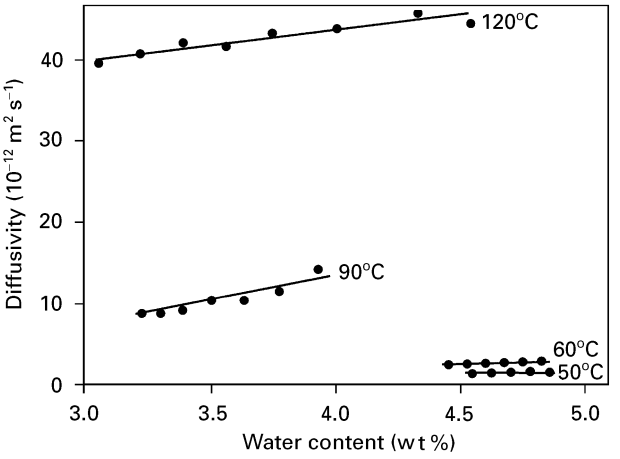

Figure 10 The effective average diffusion coefficient for water in samples dried for selected times plotted against the average water content of the samples at those times. There is a clear trend for the diffusivity to decrease with decreasing water content. However, this trend is not different for samples in the glassy state ($T = 50\,^{\circ}\mathrm{C}$ and $60\,^{\circ}\mathrm{C}$, $< T_g$) and in the rubbery state ($T = 90\,^{\circ}\mathrm{C}$ and $120\,^{\circ}\mathrm{C}$, $> T_g$).

4.5. Dependence of diffusion coefficient on water content

Applying Equation 4 at selected times as drying of a sample proceeds, the average diffusivity up to those times can be obtained. In Fig. 10 such average values are plotted against the average water content of the sample at the corresponding times. It is evident that the average diffusivity can decrease by as much as 40% in the drying range used in these experiments. With diffusion being rate-limiting, the water content of drying samples is highly non-uniform, and therefore fitting of the curves in Fig. 10 has not been attempted. At the lower drying temperatures shown in the figure ($50\,^{\circ}\mathrm{C}$ and $60\,^{\circ}\mathrm{C}$) the average water content of the samples throughout the drying is always below that corresponding to the glass transition, i.e., the samples are always in the glassy state. For the higher drying temperatures ($90\,^{\circ}\mathrm{C}$ and $120\,^{\circ}\mathrm{C}$) the samples are always in the rubbery state. It is clear that there is no significant difference between the dependences of diffusivity on water content in these two states.

5. Discussion

The non-linearity of the plots in Fig. 6 clearly shows that diffusion in the sample, not evaporation, is the rate-limiting step in drying Ficoll–water mixtures. There is no strong dependence of diffusivity on water content (Fig. 10). Furthermore (Figs 7 and 10), the diffusion behaviour (i.e. the dependence of diffusivity on temperature and on water content) is not different in the glassy and rubbery states on either side of the glass transition. Thus Fickian diffusion kinetics (Equation 4) apply throughout the drying process, and the analysis is comparatively straightforward. The temperature dependence of the water diffusivity is Arrhenian. This temperature dependence, and the same behaviour extending throughout the glass-transition region, show that the mobility of the water is unaffected by the mobility of the carbohydrate

(which would be expected to take the form shown in Fig. 1). The independence of the water from the carbohydrate mobility is in accord with the findings for small diffusing species in polymers [8].

The activation energy for water diffusion in Ficoll–water has been found in this work to be $57 \pm 5\,\mathrm{kJ\,mol^{-1}}$. This is just below the range, 65 to $190\,\mathrm{kJ\,mol^{-1}}$, quoted by Karmas *et al.* [20] for non-enzymatic browning reactions above T_g in foods. It is higher than the activation energy for self-diffusion in liquid water in the same temperature range, 18 to $24\,\mathrm{kJ\,mol^{-1}}$ [21], but similar to the activation energy of $70\,\mathrm{kJ\,mol^{-1}}$ found for diffusion of water in maltose–water [5].

The absolute values of water diffusivity (Fig. 8) are also (extrapolated to the same temperature) very similar to those found by Parker and Ring [5] for maltose–water; both in [5] and in the present work the drying temperatures are close to T_g. Even at the lowest drying temperature, 50 °C, the water is quite mobile: $D = 2 \times 10^{-13}\,\mathrm{m^2\,s^{-1}}$, corresponding to a diffusion distance $(2Dt)^{1/2}$ of 0.4 μm in 1 h. This is four to five orders of magnitude less than the self-diffusion in bulk water at the same temperature [21].

The Arrhenian temperature dependence of diffusivity D is of course described by

$$D = D_0 \exp\left(\frac{-E_a}{RT}\right), \tag{5}$$

where E_a is the activation energy and R the gas constant. If the mechanism of diffusion is by simply activated jumps, then the pre-exponential factor is expected to be approximated by

$$D_0 = \frac{1}{6}\nu\lambda^2, \tag{6}$$

where ν is the Debye frequency, and λ is the jump distance, similar to the molecular diameter. Taking $\nu = 10^{14}$ Hz, and estimating $\lambda = 0.385$ nm from the molar volume of water, gives $D_0 = 2.5 \times 10^{-6}\,\mathrm{m^2\,s^{-1}}$. The value of D_0 can also be estimated from the data in Fig. 8. Typically, and in the present case also, such estimations are subject to very large error because of the limited temperature range in which the diffusivity data are acquired and the long extrapolation required. The value obtained is $2.4 \times 10^{-4}\,\mathrm{m^2\,s^{-1}}$. This represents, for D_0, rather good agreement between measured and theoretical values. The implication is that the diffusion of water in the glassy carbohydrate can be regarded as that of an interstitial solute in a rigid matrix. If there were coupling between the mobility of the water and that of the carbohydrate, non-Arrhenian behaviour (e.g. Fig. 1) would be observed, with anomalous values of D_0 arising from Arrhenian fitting.

The results enable some conclusions to be drawn about the optimum procedures for preservation by drying. As pointed out by Pikal *et al.* [14], a higher temperature may not necessarily lead to more decomposition of a product in a carbohydrate matrix because of the shorter drying time; the key comparison is between the temperature dependences of drying rate and decomposition rate. As shown in this work, the drying rate has an Arrhenian temperature dependence through T_g. However, the temperature dependence of the product degradation rate may change markedly with the physical state of the stabilizing matrix. Drug or protein molecules, being much larger than water molecules, have diffusivities much more closely related to the viscosity of the matrix in which they are embedded. As the viscosity decreases on heating through the glass transition, the degradation of the product is able to proceed much more rapidly. For example the non-enzymatic browning (Maillard) reaction important in foods [20], is barely detectable below T_g, but proceeds rapidly (much faster than predicted by an extrapolation of the sub-T_g Arrhenian kinetics) above T_g. Hence for optimum drying without degradation the stable glassy state should be maintained, the system being held at or just below T_g. As drying proceeds, the T_g increases and the drying temperature may be increased. However, fast ramping of temperature is not desirable as it can generate large temperature gradients. As shown by Shalaev and Franks [22], chemical reactions may be prevented by drying in the region of T_g.

6. Conclusions

The kinetics of evaporative drying have been measured for a carbohydrate-based system (Ficoll–water) in the glassy and rubbery states near the glass transition (water content 3 to 5.5 wt %). The rate of drying is controlled not by the evaporation at the sample surface, but by the rate of transport of water in the sample. This transport is by bulk diffusion and Fickian kinetics are observed, consistent with the diffusivity decreasing only weakly with decreasing water content. The diffusivity has an Arrhenian temperature dependence with activation energy $57 \pm 5\,\mathrm{kJ\,mol^{-1}}$. The physical state, glass or rubber, of the samples can be determined from DSC data giving T_g as a function of water content. However, the change of state at T_g has no effect on the diffusion behaviour (the dependences of D on temperature and on water content). Water appears to be an interstitial solute with its mobility decoupled from that of the carbohydrate matrix; in this way the water retains significant mobility well below T_g. Since the mobility of the carbohydrate is important in some degradation processes, it is concluded that for most effective preservation (including, for example, stabilization of an embedded labile pharmaceutical) drying should be carried out at temperatures just below T_g.

Acknowledgements

The authors gratefully acknowledge financial support from Trinity College, Cambridge.

References

1. F. FRANKS, R. H. M. HATLEY and S. F. MATHIAS, *Pharm. Technol. Int.* **Oct.** (1991) 24.
2. U.S. Patent 3,300,474, 1967.

3. D. GIRLICH, Ph.D. thesis, University of Regensburg (1991).
4. C. A. OKSANEN and G. ZOGRAFI, *Pharm. Res.* **10** (1993) 791.
5. R. PARKER and S. G. RING, *Carbohydrate Res.* **273** (1995) 147.
6. C. A. ANGELL, *J. Phys. Chem. Solids* **49** (1988) 863.
7. J. D. FERRY, "Viscoelastic properties of polymers", 3rd edition (Wiley, New York, 1980).
8. D. EHLICH and H. SILLESCU, *Macromolecules* **23** (1990) 1600.
9. T. SOESANTO and M. C. WILLIAMS, *J. Phys. Chem.* **85** (1981) 3338.
10. D. GIRLICH and H.-D. LÜDEMANN, *Z. Naturforschung* **48c** (1993) 407.
11. Y. ROOS and M. KAREL, *Biotechnol. Prog.* **6** (1990) 159.
12. T. NOEL, R. PARKER and S. G. RING, in "Food macromolecules and colloids", edited by E. Dickinson and D. Lorient (Royal Society of Chemistry, Cambridge, 1995) p. 543.
13. R. B. LESLIE, P. J. CARILLO, T. Y. CHUNG, S. G. GILBERT, K. HAYAKAWA, S. MAROUSIS, G. D. SARAVACOS and M. SOLBERG, in "Water relationships in food", edited by H. Levine and L. Slade (Plenum, New York, 1991) p. 365.
14. M. J. PIKAL, S. SHAH, M. L. ROY and R. PUTMAN, *Int. J. Pharmaceutics* **60** (1990) 203.
15. N. THOMAS and A. H. WINDLE, *Polymer* **19** (1978) 255.
16. R. H. M. HATLEY, F. FRANKS and M. GREEN, *Thermochim. Acta* **156** (1989) 247.
17. J. ZARZYCKI, "Glasses and the vitreous state", (Cambridge University Press, Cambridge, 1991).
18. J. CRANK,"The mathematics of diffusion", 2nd edition (Oxford University Press, Oxford, 1975).
19. P. G. SHEWMON, "Diffusion in solids", 1st edition (McGraw-Hill, New York, 1963) p. 16.
20. R. KARMAS, M. P. BUERA and M. KAREL, *J. Agric. Food Chem.* **40** (1992) 873.
21. C. A. ANGELL, in "Water: a comprehensive treatise", vol. 7, edited by F. Franks (Plenum, New York, 1982), ch. 1, p. 44.
22. E. Y. SHALAEV and F. FRANKS, *J. Chem. Soc. Faraday Trans.* **91** (1995) 1511.

Received 23 April
and accepted 21 May 1996